JOURNAL OF VIROLOGY, Nov. 1996, p. 7641–7653 Vol. 70, No. 11
0022-538X/96/$04.00+0

Inducible Expression of the Vaccinia Virus A17L Gene Provides a Synchronized System To Monitor Sorting of Viral Proteins during Morphogenesis

DOLORES RODRÍGUEZ, CRISTINA RISCO, JUAN RAMÓN RODRÍGUEZ, JOSÉ L. CARRASCOSA, AND MARIANO ESTEBAN*

Centro Nacional de Biotecnología, Consejo Superior de Investigaciones Científicas, Campus Universidad Autónoma, 28049 Madrid, Spain

Received 15 April 1996/Accepted 6 August 1996

The vaccinia virus (VV) A17L gene encodes a 21- to 23-kDa virion component that forms a stable complex with the 14-kDa envelope protein (A27L gene). In a previous report, we described the construction of a VV recombinant, VVindA17L, in which the expression of the A17L gene is inducibly regulated by isopropyl-β-D-thiogalactoside (IPTG). We demonstrated that shutoff of the A17L gene results in a blockade of virion morphogenesis at a very early stage (D. Rodríguez, M. Esteban, and J. R. Rodríguez, J. Virol. 69:4640–4648, 1995). In the present study, we show that virus growth is restored if the inducer is provided not later than 6 h postinfection. Immunofluorescence and immunoelectron microscopy analysis of VVindA17L-infected cells revealed that in the absence of the 21- to 23-kDa protein, the 14-kDa protein is distributed throughout the cytoplasm. After IPTG addition, the 14-kDa protein can be detected around viral factories and immature virions; at later times, it localizes in the external membranes of intracellular mature virions. Immunoelectron microscopy with anti-21- to 23-kDa antibodies showed that soon after induction, the protein accumulates in membranes of the rough endoplasmic reticulum and in the nuclear envelope. With time, the protein localizes in viral crescents and subsequently associates to the membranes of immature and intracellular mature virions. These results are consistent with a model in which the 21- to 23-kDa protein would be synthesized at the endoplasmic reticulum, from where the protein could be translocated to the membranes of the intermediate compartment to generate the precursors of the viral membranes. Also, these results argue that 14-kDa envelope protein becomes posttranslationally associated to viral membranes through its interaction with the 21-kDa protein.

Vaccinia virus (VV) is the prototype member of the *Poxviridae* family, a group of DNA viruses that replicate entirely in the cytoplasm of the host cell (19). The large viral DNA genome encodes about 200 proteins, many of which are assembled into the virions. The morphologically distinct stages of the assembly process have been described in detail after electron microscopy examination (5, 6, 14). During the course of infection, the first distinguishable viral structures are crescent-shaped membranes formed around electron-dense areas termed viral factories. Recent investigations indicate that these rigid structures are derived from membranes of the intermediate compartment (IC) between the endoplasmic reticulum (ER) and the Golgi complex (37). As assembly progresses, spherical immature virions (IVs) are formed and will evolve to produce the characteristic brick-shaped virions, recently named intracellular mature virions (IMVs), which constitute the first infectious form of the virus. Some of these viral particles are wrapped by a membrane cisternae derived from the trans-Golgi network (34). By fusion with the plasma membrane, these virions lose the outermost membrane and are released from the cell. These extracellular enveloped virions (EEVs), which expose on the external surface several proteins not present in IMVs (9, 15, 24, 25), largely contribute to virus spread in cultured cells and in infected animals (1, 4, 26, 27).

The molecular events leading to the formation of the complex virion structures are still largely unknown. It has been established that proteolytic processing of several virion components is an essential step in virion maturation that occurs at a late stage (17, 20, 41). In addition, two approaches are used to elucidate the function of VV proteins in the morphogenetic process. One is based on the characterization of temperature-sensitive mutants showing defects in assembly, and the other relies on the generation of inducer-dependent conditional mutants in which the gene of interest can be conveniently shut off or inducibly expressed. By using these two approaches, it is possible to identify essential proteins for VV morphogenesis and define at which step of this process they are required. Most of the protein involved in morphogenesis identified so far are required for either the transition from IV to IMV (11, 16, 28, 45, 48) or the envelopment process leading to EEV formation and/or release (2, 3, 8, 10, 23, 33, 35, 46). However, very little is known about proteins required for the initial events in morphogenesis and specifically for the generation of viral membranes. In this regard, it is known that p65 (D13L gene) is required for the formation of the crescent-shaped membranes. It was first shown that p65 is the target of rifampin (18, 40), a drug that reversibly interrupts VV morphogenesis (21, 22). In the presence of rifampin, irregularly shaped membranes accumulate around electron-dense structures known as rifampin bodies (13). Moreover, the same structures are produced when p65 protein synthesis is inhibited (49). In addition, it has been recently reported that a 52-kDa protein kinase (F10 gene) is required at an early stage of virion morphogenesis (39, 42). Consequently, it has been suggested that protein phosphorylation might be an essential function at least in the initial stages of the assembly process.

We have previously identified a 21-kDa protein that interacts with the 14-kDa envelope protein (A27L gene) (32). The 21-kDa protein is the processed form of the 23-kDa precursor

* Corresponding author. Phone: 34-1-585-4503. Fax: 34-1-585-4506. Electronic mail address: mesteban@samba.cub.uam.es.

encoded by the A17L gene (32). We have also described the generation of a VV recombinant, VVIndA17L, in which the expression of the A17L gene can be inducibly regulated by isopropyl-β-D-thiogalactopyranoside (IPTG) (31). Using this system, we demonstrated that in the absence of the 21- to 23-kDa protein, virion morphogenesis is arrested at a very early stage, prior to the formation of the crescent-shaped membranes. Under these conditions, granular electron-dense bodies are the only viral structures observed in the cytoplasm of the infected cell. A similar A17L-inducible mutant virus exhibiting the same phenotype has been recently reported (47). On the basis of these results, we proposed that 21- to 23-kDa protein is involved in the generation of viral membranes from membranes of the IC and that this protein might be targeted to the membranes of the IC.

To determine the localization of the 21- to 23-kDa protein during VV infection, we took advantage of the inducible VVindA17L viral system, in which morphogenesis can be blocked at a very early stage. In this report, we show that the morphogenesis blockade can be efficiently reverted if the inducer IPTG is provided 6 to 8 h postinfection (hpi). We have used this inducible system to monitor by immunoelectron microscopy the subcellular localization of the 21- to 23-kDa and 14-kDa envelope proteins to characterize their incorporation into viral structures.

MATERIALS AND METHODS

Cells and viruses. African green monkey kidney cells (BSC-40) and HeLa cells were grown in Dulbecco's modified Eagle's medium (DMEM) supplemented with 10% newborn calf serum (NCS). VV strain WR was propagated and titrated in BSC-40 cells. Recombinant virus VVindA17L was grown in BSC-40 cells in the presence of 2 mM IPTG.

Antisera. The anti-14-kDa protein rabbit polyclonal antiserum has been previously described (7). Two rabbit polyclonal antisera specific for the 21- to 23-kDa protein were used: (i) an antiserum raised against a C-terminal fragment (amino acids [aa] 136 to 203) (43), provided by D. E. Hruby, and (ii) an antiserum against a synthetic peptide corresponding to aa 193 to 203, produced by immunization of rabbits with the purified peptide coupled to keyhole limpet hemocyanin. The rhodamine-conjugated goat anti-rabbit antibody was purchased from Organon Teknika.

Plaque assays. Confluent monolayers of BSC-40 cells seeded in a 12-well plate were infected with 200 PFU of VVindA17L. The inoculum was removed after 1 h, and DMEM containing 2% NCS was added to the infected cells, with or without 2 mM IPTG. At 2, 4, 6, 8, and 24 hpi, IPTG was removed from individual cultures by washing the wells twice with DMEM and overlaying them with fresh DMEM containing 2% NCS. At the same time points, IPTG was added to previously untreated cultures. Two control wells were maintained in the absence or presence of IPTG for the entire infection period. To avoid the formation of secondary plaques in all of these cultures, the medium was replaced at 24 hpi by a mixture consisting of DMEM, 0.9% Bacto Agar, and 2% NCS, containing or lacking IPTG. At 48 hpi, the medium was removed and the monolayers were stained with 1% crystal violet in 2% ethanol.

One-step virus growth curves. Confluent monolayers of HeLa cells were infected with VVindA17L at a multiplicity of infection of 2.5 PFU per cell. After 1 h, the inoculum was removed and the cells were washed with fresh DMEM and overlaid with DMEM supplemented with 2% NCS. IPTG (2 mM) was added 1 h after the adsorption period or at 2, 4, 6, 8, or 24 h. For IPTG withdrawal, cultures that were treated with the inducer after the first hour of infection were washed with DMEM at 2, 4, 6, 8, or 24 hpi and overlaid with 2% NCS containing medium. Cells were harvested at 24 hpi except those to which IPTG was added or withdrawn at 24 hpi, which were maintained in culture for another 24 h. Progeny viruses were titrated by plaque assay on monolayers of BSC-40 cells in the presence of IPTG.

Metabolic labeling of viral proteins and immunoprecipitation analysis. BSC-40 cells were infected (5 PFU per cell) with VVindA17L in the absence or presence of IPTG (5 mM). At 6 hpi, cells were washed with methionine-free DMEM and incubated in the same medium with or without IPTG for 10 min. After this period, all cultures except one were treated with 5 mM IPTG and cells were immediately labeled by adding 100 μCi of [^{35}S]methionine per ml to the medium. At the indicated times postinfection, cells were placed on ice, washed three times with phosphate-buffered saline (PBS), collected, and resuspended in immunoprecipitation lysis buffer (20 mM Tris-HCl [pH 8.0], 80 mM NaCl, 20 mM EDTA, 1% Nonidet P-40) containing protease inhibitors (bacitracin [2 mg/ml], trypsin inhibitor [2 mg/ml], 1 mM phenylmethylsulfonyl fluoride, and leupeptin [10 mg/ml]). Cell extracts were maintained for 30 min on ice, sonicated, and clarified by centrifugation at 10,000 × *g* for 5 min. The supernatants were immunoprecipitated with specific antibodies as previously described (32). After being washed, the immunoprecipitates were resuspended in 2× sample buffer (1.25 M Tris-HCl [pH 6.8], 0.2% sodium dodecyl sulfate [SDS], 1% bromophenol blue, 10% 2-β-mercaptoethanol). Samples were boiled for 3 min and resolved by SDS-polyacrylamide gel electrophoresis (PAGE). The gels were dried, and the proteins were visualized after autoradiography.

Immunofluorescence microscopy. HeLa cells grown on coverslips were infected with either VV strain WR in the absence or presence of rifampin (100 μg/ml) or VVindA17L in the absence or presence of IPTG (2 mM). At 8 hpi, cells were washed with PBS and fixed with 2% paraformaldehyde in 100 mM sodium phosphate buffer (pH 7.4) for 30 min. Cells were then washed with PBS, treated with 50 mM NH_4Cl for 10 min, and permeabilized with 2% Triton X-100 in PBS for 5 min. After being washed with PBS, coverslips were blocked for 30 min with a solution containing 20% fetal calf serum (FCS) and 0.5% Tween 20 in PBS. Cells were then incubated for 1 h with the anti-14-kDa protein rabbit polyclonal serum or with the anti-21- to 23-kDa protein (aa 193 to 203) serum raised against a C-terminal peptide diluted 1:500 or 1:250, respectively, in blocking solution. The coverslips were rinsed three times with PBS and incubated with the secondary antibody conjugated with rhodamine. To stain nuclear and viral DNA, Hoechst stain (5 μg/ml) (12) was applied together with the secondary antibody. After 30 min of incubation, the coverslips were extensively washed with PBS and mounted with Mowiol on glass slides. Preparations were examined with an Axiophot microscope (Zeiss).

Immunoelectron microscopy. (i) Immunogold detection of VV proteins on sections of infected cells. Cultures of HeLa cells were infected at a multiplicity of infection of 5 PFU per cell with the recombinant virus VVindA17L in the absence of IPTG. At 6 hpi, IPTG (2 mM) was added to some cultures for 2, 4, or 18 h. At the times indicated, the supernatant was removed from the cultures and the cell monolayers were submitted to a mild fixation with a solution of 4% paraformaldehyde containing 0.1% glutaraldehyde in PBS. Fixed cells were then removed from the dishes with a plastic pipette and transferred to Eppendorf tubes. After centrifugation in a microcentrifuge and washing with PBS, the pellets were processed for embedding in Lowicryl K4M at low temperature as previously described in detail (30). Thin sections of the samples were collected in gold grids covered with Formvar and carbon and processed for immunogold labeling as previously described (29, 30).

Immunogold localization of the VV 21- to 23-kDa and 14-kDa proteins on sections of infected cells was carried out with polyclonal antisera raised against a synthetic peptide (aa 193 to 203) or a fragment of the 21- to 23-kDa protein (aa 136 to 203) and a polyclonal serum against the 14-kDa protein, respectively. Immunolabeling was performed by placing the sections on drops of different solutions. After a 30-min incubation with Tris buffer-gelatin (TBG) (30 mM Tris-HCl [pH 8.0] containing 150 mM NaCl, 0.1% bovine serum albumin, and 1% gelatin) to block nonspecific binding of the antibodies to the samples, sections were floated for 90 min on a drop of the specific primary antiserum, diluted in TBG (1:200 for the rabbit anti-21-kDa protein [aa 136 to 203] antiserum, 1:100 for the rabbit anti-21-kDa protein [aa 193 to 203] antiserum, and 1:150 for the rabbit anti-14-kDa protein antiserum). After jet washing with PBS, grids were floated on 4 drops of the saturation buffer and incubated 10 min on the last drop before a 45-min incubation with the secondary antibody (goat anti-rabbit immunoglobulin G or goat anti-mouse immunoglobulin G) conjugated with colloidal gold of 5 or 10 nm. Washing was repeated as before, and grids were then floated on several drops of distilled water before staining with a solution of saturated uranyl acetate for 20 min. After washing with distilled water and air drying, samples were studied in a JEOL 1200EX II electron microscope.

(ii) Immunogold labeling of isolated virions for detection of VV proteins exposed on the surface of IMVs. Purified IMVs were attached to electron microscopy copper grids covered with Formvar and carbon and previously made hydrophilic by glow discharge. These grids were placed on drops of a concentrated IMV suspension, and virions were adsorbed for 5 min. After removal of the excess liquid by touching the edge of the grid with filter paper, immunolabeling of virions was performed as previously described (29). After a 10-min incubation in TBG, grids were transferred to drops of the corresponding diluted antisera and incubated for 20 min. After washing with several drops of TBG, the grids were incubated for 20 min with a 10-nm colloidal gold conjugate of goat anti-rabbit immunoglobulin G (diluted 1:30 in TBG). Grids were then washed by floating them on 4 drops of TBG and 4 more drops of distilled water before negative staining with a 2% solution of uranyl acetate. Samples were finally studied by electron microscopy.

RESULTS

Reversibility of virus growth arrest by addition of IPTG at different times after infection. We have previously shown that the 21- to 23-kDa protein is essential for the generation of progeny virus (31). Both virus yields and formation of viral plaques are dramatically reduced in cells infected with VVindA17L in the absence of IPTG. Thus, to investigate if this effect was reversible, we performed one-step virus growth

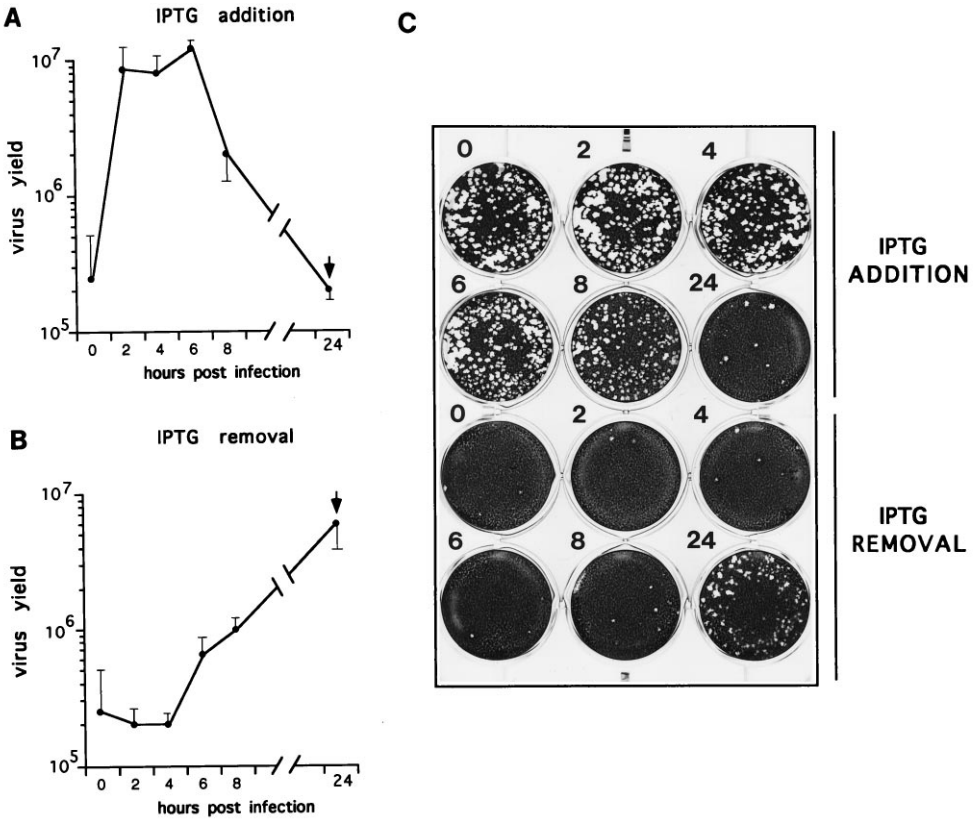

FIG. 1. Effect of addition and removal of IPTG on VVindA17L virus growth. (A and B) One-step growth curves. HeLa cells were infected in duplicates with VVindA17L at a multiplicity of infection of 2.5 PFU per cell in the absence (A) or presence (B) of IPTG (2 mM). At the indicated times postinfection, IPTG was either added to the wells (A) or removed (B). The zero time points represent cultures that were collected just after the 1-h adsorption period, to establish the background titer due to the input virus. All other cultures were collected at 24 hpi, except those to which IPTG was either added or washed out at 24 hpi (indicated by the arrow), which were collected at 48 hpi. Virus yields were determined by titration on BSC-40 cells in the presence of 2 mM IPTG. (C) Confluent monolayers of BSC-40 cells were infected with 200 PFU of VVindA17L. After a 1-h adsorption period, DMEM supplemented with 2% NCS was added to the wells. The six wells in the lower part of the plate also received IPTG (2 mM). At 0, 2, 4, 6, 8, and 24 hpi (as indicated by the numbers), IPTG (final concentration, 2 mM) was either added to the wells (upper half of each plate) or withdrawn from the wells (lower part of each plate). At 24 hpi, all wells were overlaid with a mixture containing DMEM, 0.9% Bacto Agar, and 2% NCS containing or lacking IPTG (2 mM). At 48 hpi, the monolayers were stained with 1% crystal violet.

curves, using cells infected with VVindA17L after addition of IPTG at different times postinfection. Figure 1A shows the results of viral yields from cultures infected for 24 h. While maximum viral yields were obtained when IPTG was provided at or before 6 hpi, a significant drop in virus production was observed when IPTG was added at 8 hpi. Moreover, virus yields from cultures that were first treated with IPTG at 24 hpi and maintained for another 24 h period remained at the background level. Removal of IPTG from the culture medium at early times (2 to 4 hpi) completely abolished virus production. A slight increase in virus yields was observed when IPTG was removed at 6 or 8 hpi (Fig. 1B). As for IPTG addition, washing out of the inducer at 24 hpi does not have a significant effect on the virus yields obtained after another 24-h infection period compared with parallel cultures that were maintained in the continuous presence of IPTG (data not shown).

Similarly, we investigated the effects on VVindA17L plaque formation of both addition and withdrawal of IPTG at different times postinfection. As shown in Fig. 1C, the numbers of plaques were roughly the same when IPTG was added after virus adsorption and at up to 8 hpi. A dramatic reduction in the number of plaques was observed when IPTG was added at 24 hpi. Conversely, the number of plaques was reduced to background levels when IPTG was washed out of the culture medium during the first 8 h of infection. However, plaques were readily formed when IPTG was withdrawn at 24 h, although they were reduced to some extent in both number and size compared with plaques formed in the continuous presence of IPTG. This result indicates that continuous production of the 21- to 23-kDa protein is required to establish subsequent rounds of viral replication in the neighboring cells.

Taken together, the results presented show that inhibition of virus growth in VVindA17L-infected cells is reversible, but only if the inducer is provided within a period of time from virus adsorption up to 6 hpi, which is about the time when the switch between early and late virus protein synthesis occurs.

Time course of 21- to 23-kDa protein synthesis after IPTG addition. Since high virus yields were still produced when the inducer was added at 6 hpi, it was of interest to examine the time course of 21- to 23-kDa protein synthesis and its interaction with 14-kDa protein under these conditions. Thus, cells infected with VVindA17L (Fig. 2A, lanes 6 to 10) and treated with IPTG at 6 hpi were labeled with [^{35}S]methionine for different time periods. For comparison, cultures of VVindA17L-infected cells to which IPTG was added immediately after virus adsorption were also labeled (Fig. 2A, lanes 1 to 4). Proteins were immunoprecipitated with antibodies specific to the 21- to 23-kDa protein raised against a synthetic peptide (aa 193 to 203). As we have previously reported (31), expression of the 21- to 23-kDa protein in cells infected with VVindA17L is

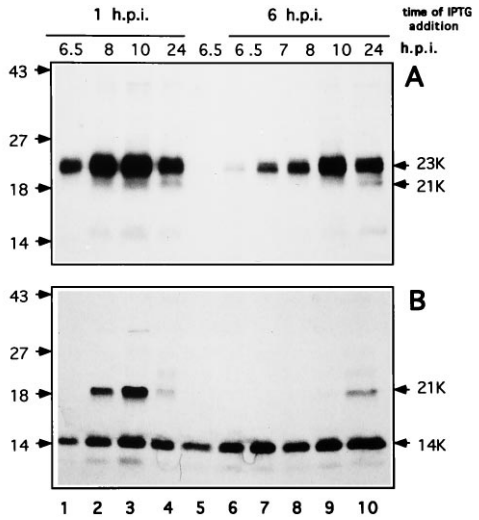

FIG. 2. Synthesis of the 21- to 23-kDa protein after induction with IPTG. (A) Immunoprecipitation of the 21- to 23-kDa protein with the antiserum against a C-terminal peptide of the protein. BSC-40 cells were infected with VVindA17L and treated with IPTG (5 mM) just after a 1-h adsorption period (lanes 1 to 4) or at 6 hpi (lanes 6 to 10). One culture was uninduced (lane 5). Cells were metabolically labeled with [^{35}S]methionine (100 μCi/ml) from 6 hpi to the times indicated at the top. After the labeling period, cells were harvested, and cell extracts were immunoprecipitated with the anti-21- to 23-kDa protein serum raised against a synthetic peptide corresponding to the C-terminal 10 aa of the protein. The immunoprecipitated products were separated by SDS-PAGE (12% polyacrylamide gel) and visualized after autoradiography of the dried gel. (B) Coimmunoprecipitation of the 14-kDa and 21-kDa proteins with a polyclonal serum directed against the 14-kDa protein. The extracts used for immunoprecipitation in panel A were also immunoprecipitated with anti-14-kDa protein antibodies. The positions of 23-, 21-, and 14-kDa proteins are indicated on the right; molecular weight markers are indicated on the left (in kilodaltons).

dependent of the addition of the inducer. Figure 2A shows that in cells infected for 6.5 h under nonpermissive conditions, the 21- to 23-kDa protein was completely absent (lane 5), but as soon as 30 min after IPTG addition, newly synthesized protein could be observed (lane 6), and the amount of 21- to 23-kDa protein rapidly increased with time after induction (compare lanes 7 to 9).

The amount of 21- to 23-kDa protein accumulated by 8 and 10 hpi was slightly higher in infected cells continuously maintained in IPTG-containing medium (compare lanes 2 and 8 and lanes 3 and 9). At later times postinfection, there was a decrease in the quantity of 21- to 23-kDa protein both in cultures continuously treated with the inducer and in cultures to which IPTG was added at 6 hpi (lanes 4 and 10, respectively).

We have also reported that the 21-kDa cleaved product of the 23-kDa precursor protein interacts with the 14-kDa envelope protein (32). Both proteins can be coprecipitated with antibodies against the 14-kDa protein. Thus, to determine if this 14-kDa–21-kDa protein interaction can be established after induction of 21-kDa protein synthesis late in infection, the same cell extracts were immunoprecipitated with antibodies specific for the 14-kDa protein. As shown in Fig. 2B (lanes 1 to 3), under permissive conditions, the interaction could be observed soon after 21-kDa protein synthesis had begun. However, in cultures that were first treated with IPTG at 6 hpi, complex formation could be clearly observed at late times (24 hpi) (lane 10), although trace amounts of 21-kDa protein coprecipitated at 4 h postinduction could also be observed with longer exposures of the autoradiogram (data not shown).

These results clearly show that expression of the A17L gene can be restored when the inducer is provided at 6 hpi. However, the formation of the 14-kDa–21-kDa protein complex is greatly delayed under these conditions in which the synthesis of both 14- and 21-kDa proteins is not simultaneous.

Immunofluorescence analysis of VVindA17L-infected cells under permissive and nonpermissive conditions. From our earlier studies, we suggested that the 21-kDa protein may serve to anchor the 14-kDa protein to the envelope of IMVs (31, 32). Thus, it was of interest to determine the intracellular localization of the 14-kDa protein in the absence of the 21- to 23-kDa protein, and consequently virion morphogenesis was blocked.

The distribution of both 21- and 14-kDa proteins was first analyzed by immunofluorescence in HeLa cells infected for 8 h with VVindA17L, in the absence or in the continuous presence of IPTG. For comparison, cells infected with WR in the absence or presence of the assembly inhibitor rifampin were also examined. In WR-infected cells, antibodies against the 21- to 23-kDa protein showed a reticular labeling pattern throughout the cytoplasm (Fig. 3A) that possibly corresponds to ER labeling. In addition, the areas in the vicinity of the nucleus corresponding to viral factories, as shown by Hoechst DNA staining (Fig. 3C), were strongly stained. Moreover, the nuclear membrane was clearly labeled with this antibody. In cells infected with VVindA17L under permissive conditions, labeling with anti-21- to 23-kDa protein was weaker than in WR-infected cells as a result of reduced levels of A17L gene expression as noted earlier (31). The labeling was mostly confined to viral factories (Fig. 3F). Reticular staining of the cytoplasm and the nuclear periphery was also evident in these cells (Fig. 3F). A similar pattern of staining was observed in WR-infected cells treated with rifampin, although reticular labeling of the cytoplasm was more pronounced in the latter (Fig. 3B). As expected, in cells infected with VVindA17L in the absence of IPTG, staining with anti-21- to 23-kDa protein antibodies was clearly diminished (Fig. 3E), although some weak labeling was observed in the proximity of the nucleus in areas that stain with the DNA dye (Fig. 3G). This is probably due to leakiness on the expression of the A17L gene.

In cells infected with either WR (Fig. 4A) or VVindA17L (Fig. 4F) under permissive conditions, anti-14-kDa protein antibodies gave a strong punctate staining all around the periphery and inside the cells. This pattern most likely is the result of recognition by the antibodies of individual IMVs as previously reported (36). When virus morphogenesis was blocked by treatment with rifampin, the anti-14-kDa protein antibodies strongly labeled areas near the nucleus (Fig. 4B) that presum-

FIG. 3. Localization of 21- to 23-kDa protein by immunofluorescence. HeLa cells were infected with VV strain WR in the absence (A and C) or presence (D) of rifamcin (Rif) or with VVindA17L in the absence (E and G) or presence (F and H) of IPTG (2 mM). At 8 hpi, cells were fixed and incubated with anti-21- to 23-kDa (aa 193 to 203) serum. Rhodamine-conjugated goat anti-rabbit antibody was applied together with the Hoechst DNA dye. The results of rhodamine labeling (A, B, E, and F) and DNA staining (C, D, G, and H) are shown. Labeling with anti-21- to 23-kDa antibodies shows a reticular staining throughout the cytoplasm and strong staining on the areas of viral factories, as detected by DNA staining (arrowheads in panel C), and around the nucleus. Reticular staining was weaker in rifampin-treated cells infected with WR (B) and in cells infected with VVindA17L in the presence of the inducer (F), but in both cases there was strong staining on the nuclear membrane and in areas near the nucleus, where rifampin bodies (arrowheads in panel B) and viral factories (arrowheads in panel F) accumulate, as determined by DNA staining (arrowheads in panels D and H, respectively). Cells infected with VVindA17L in the absence of the inducer (E) were weakly stained in the cytoplasm by the anti-21- to 23-kDa antibody, showing more intensity in areas close to the nucleus (arrowheads) that are also stained with the DNA dye (arrowheads in panel G).

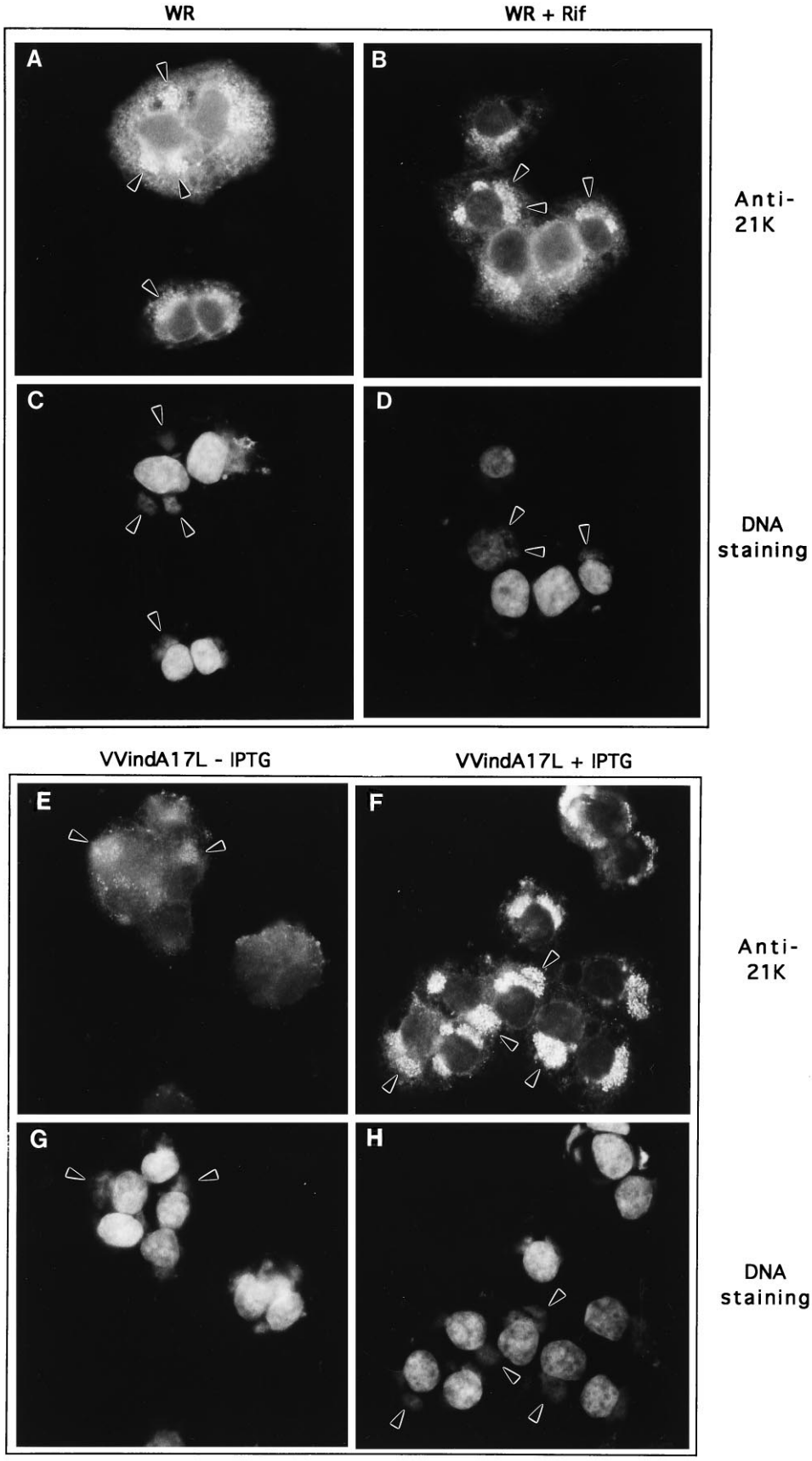
WR
WR + Rif
A
B
C
D
Anti-21K
DNA staining
VVindA17L - IPTG
VVindA17L + IPTG
E
F
G
H
Anti-21K
DNA staining

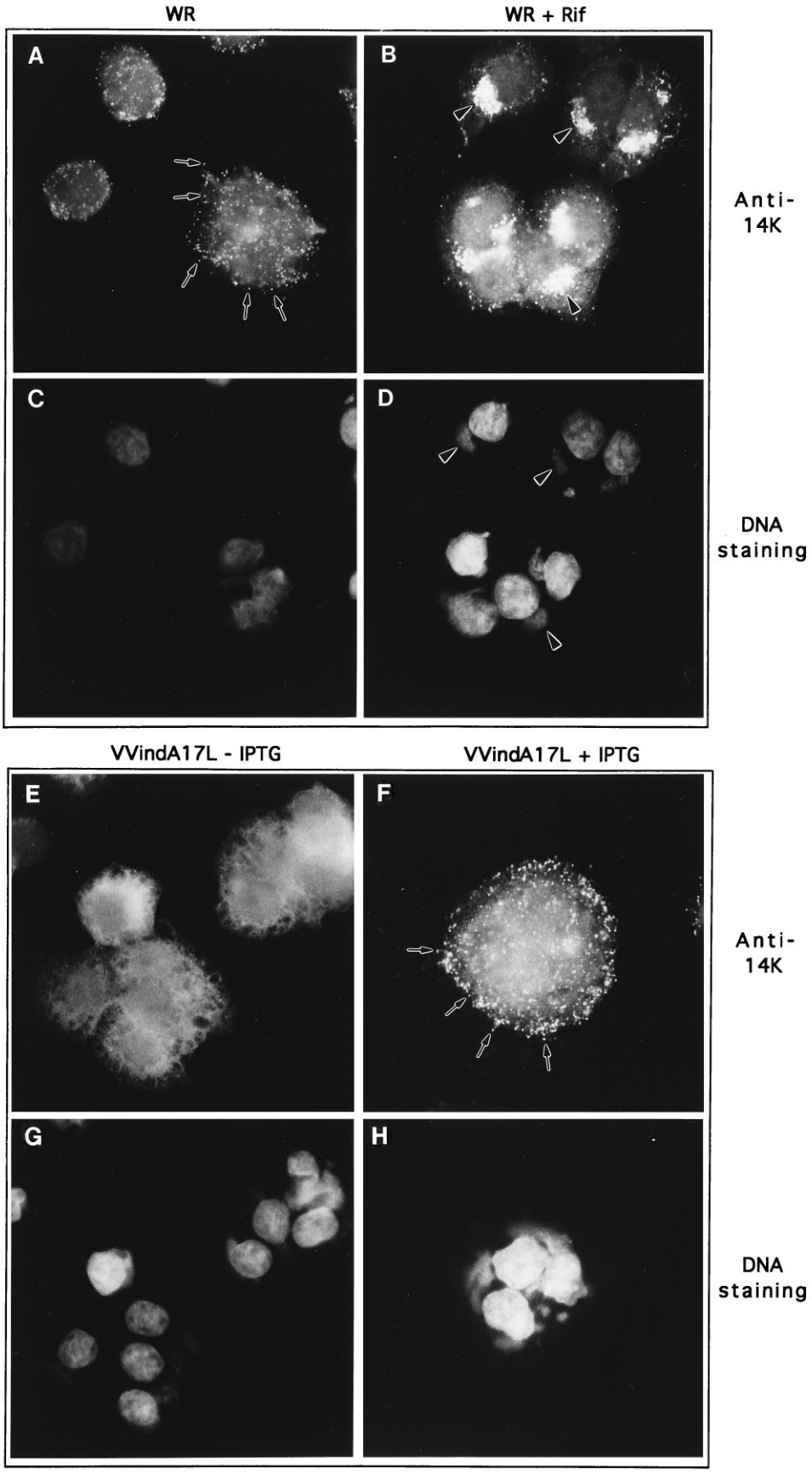
WR
WR + Rif
A
B
C
D
Anti-14K
DNA staining
VVindA17L - IPTG
VVindA17L + IPTG
E
F
G
H
Anti-14K
DNA staining

FIG. 4. Localization of the 14-kDa protein by immunofluorescence. HeLa cells infected for 8 h with WR in the absence (A and C) or presence (B and D) of rifampin or with VVindA17L in the absence (E and G) or presence (F and H) of IPTG (2 mM) were fixed and incubated with anti-14-kDa protein rabbit serum followed by a rhodamine-conjugated secondary antibody and a fluorescent DNA dye. The results of the antibody labeling (A, B, E, and F) and DNA staining (C, D, G, and H) are shown. In WR-infected cells (A) and in cells infected with VVindA17L in the presence of the inducer (F), the 14-kDa protein appears to have accumulated in strongly labeled small dots that are localized all over and around the cells (small arrowheads in panels A and F respectively) and likely correspond to mature virions. The punctate staining clearly diminishes in rifampin-treated WR-infected cells (B), but there is strong labeling in areas of accumulation of rifampin bodies (arrowheads), as determined by DNA staining (arrowheads in panel D). In cells infected with VVindA17L in the absence of the inducer, the 14-kDa protein appears dispersed throughout the cytoplasm (E).

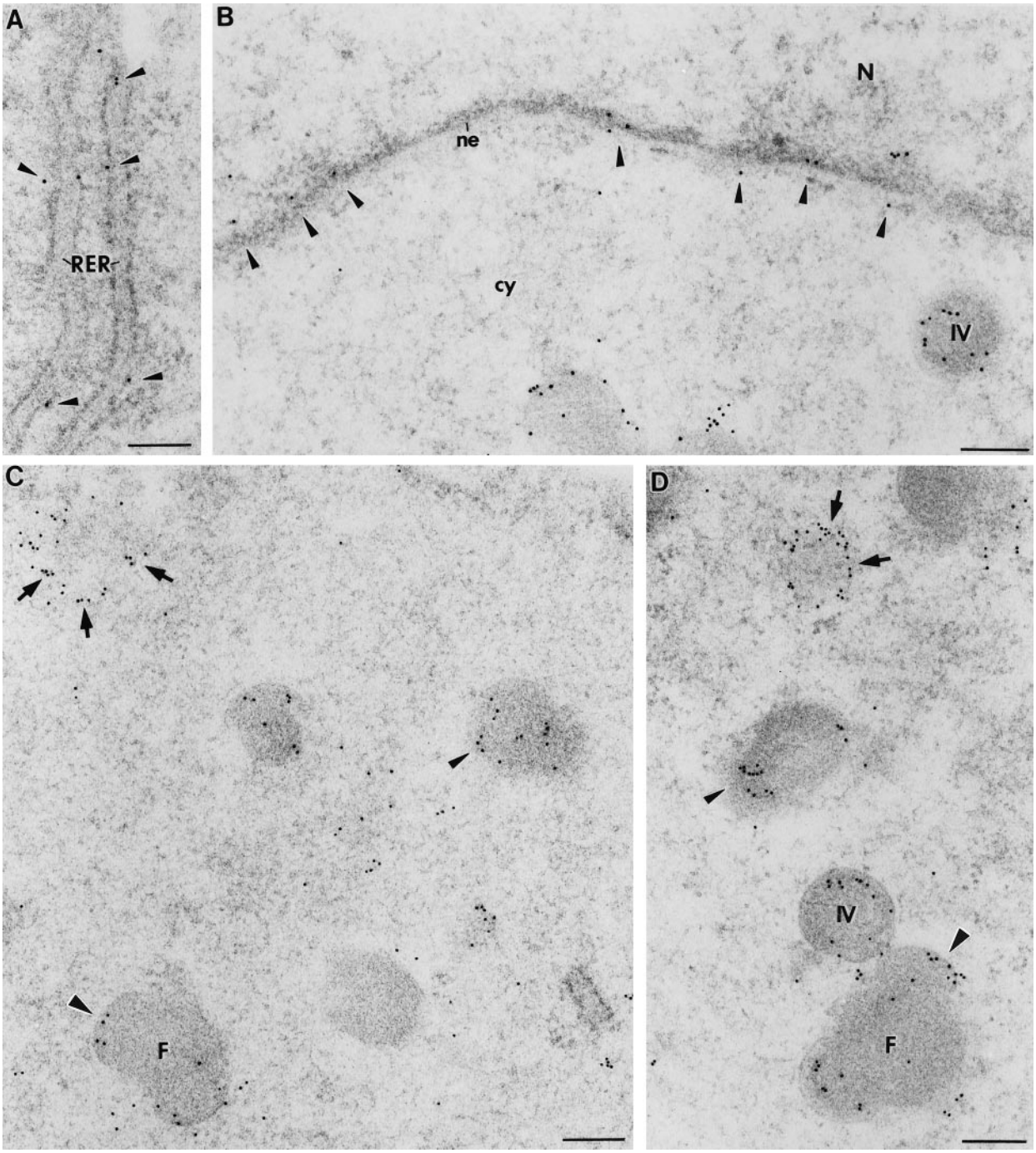

FIG. 5. Immunoelectron microscopy localization of the 21- to 23-kDa protein in cells infected with the recombinant virus VVindA17L shortly after induction of the A17L gene with IPTG. (A) After 2 h of induction, the 21- to 23-kDa protein localizes (arrowheads) in the cisternae of the RER. (B) This protein is also detected in the nuclear envelope (ne) (arrowheads). After 2 h (C) and 4 h (D), the protein is localized in particular areas of the cytoplasm, where it arranges building circles (arrows). This finding suggests that the protein molecules associate to organizing structures (potential smooth membranes). The protein is also detected on the periphery of small electron-dense masses (small arrowheads). The small viral factories (F) that start to organize have also 21- to 23-kDa molecules associated with the crescent-shaped membranes (large arrowheads). cy, cytoplasm; N, nucleus. Bars, 200 nm.

ably correspond to rifampin bodies since they were also stained with the DNA dye (Fig. 4D). Interestingly, in infected cells in which synthesis of the 21- to 23-kDa protein was repressed (VVindA17L-IPTG cells), the anti-14-kDa protein antibodies gave a diffuse staining of the cytoplasm (Fig. 4E), indicating that the 14-kDa protein was not associated with defined structures.

Localization of 21- to 23-kDa and 14-kDa proteins during the course of virus infection by immunoelectron microscopy. To establish in more detail the localization of the 21- to 23-kDa and 14-kDa proteins during the course of infection, we performed immunogold labeling and electron microscopy. HeLa cells infected with VVindA17L were either maintained in the absence of IPTG for 24 h or treated with IPTG at 6 hpi for 0.5, 1, 2, 4, and 18 h. Cells were then fixed and processed for immunoelectron microscopy.

As shown in Fig. 5, after short times of induction with IPTG (2 and 4 h), the 21- to 23-kDa protein is detected in membranes of the rough ER (RER) (Fig. 5A) and in the nuclear envelope (Fig. 5B). The protein molecules are also detected in particular areas of the cytoplasm where they arrange building circles (arrows in Fig. 5C and D), suggesting that they are associated to some structure or support, possibly smooth-walled membranes. In these infected cells, small electron-dense areas begin to form, and the 21- to 23-kDa protein localizes on their periphery. These electron-dense areas will subsequently evolve to form small viral factories (arrowheads in Fig. 5C and D). In the factories, the 21- to 23-kDa protein associates with the crescent-shaped membranes that can easily be distinguished as emerging from these large structures (Fig. 5C and D; Fig. 6A).

In immature virions, the 21- to 23-kDa protein associates with the periphery of membranes (Fig. 6B), although a more internal localization of the protein is also frequently observed in IV-like particles (Fig. 6C). These structures have the same size as the rest of the IVs, but their periphery is less electron dense and the signal associated with the 21- to 23-kDa protein is restricted to an internal layer inside the particle, clearly separated from its surface (Fig. 6C). In IMVs, the 21- to 23-kDa protein is associated with the membranes (Fig. 6D), as observed with an antiserum raised against a C-terminal fragment of the protein (aa 126 to 203). Interestingly, when the immunogold labeling is done with an antiserum raised against a shorter peptide (aa 193 to 203), the signal associated with IVs appears intense but disappears in IMVs and EEVs (Fig. 6G and H).

Because of the heterogeneity observed in the immunolabeling of ultrathin sections with antibodies against the 21- to 23-kDa protein, it was difficult to determine whether the protein is localized in the outer or inner membrane or in both membranes of the viral envelope. Thus, our next approach was to carry out immunogold labeling in purified IMVs. A clear variability in the degree of surface exposure of the 21- to 23-kDa protein was also observed in purified IMVs. We found that 12% of virions exhibit a strong surface signal associated with the protein when immunolabeled by using the anti-21- to 23-kDa protein antiserum raised against the smaller peptide (aa 193 to 203) (Fig. 6F), 78% of the virions had a weak signal (Fig. 2E), and 10% of the virions were unlabeled (not shown). As a control for IMV integrity, purified virions were processed for immunogold labeling by using a rabbit antiserum raised against the core protein of 39 kDa (7), and no surface signal was observed in this case (data not shown).

Immunolabeling with anti-14-kDa protein antibodies showed that when synthesized in the absence of virion assembly (without induction of the A17L gene), the 14-kDa protein was detected dispersed within the cytoplasm and apparently did not associate with any particular structure (Fig. 7A). This result is in agreement with the immunofluorescence results shown in Fig. 4E. After induction of viral assembly, a small amount of this protein is detected in the crescent-shaped membranes of the viral factories (Fig. 7B). Some IVs also present a small amount of 14-kDa protein incorporated in their periphery (Fig. 7C and D), but this protein binds in higher amounts to a different viral form that, as previously reported (36), probably represents an intermediate stage between the IV and the IMV (Fig. 7E). The 14-kDa protein was largely associated with IMVs, anchored to their surface and covering the entire periphery (Fig. 7F and G). The findings in Fig. 7 indicate that incorporation of the 14-kDa protein into viral structures starts at an early stage of virion formation, but higher accumulation of this protein in viral envelopes is observed at later stages.

DISCUSSION

Using an inducer-dependent conditional mutant, we have recently shown that repression of the A17L gene, which codes for a 21- to 23-kDa protein, results in a blockade of virion morphogenesis. This is apparently related to impairment in the formation of viral membranes around the virus factories (31). Extending our previous studies, in this report we have explored the possible reversibility of the morphogenesis arrest caused by repression of 21- to 23-kDa protein synthesis. By both addition and removal of IPTG from cultures of VVindA17L-infected cells, we have observed that there is a critical period, between 6 and 8 hpi, after which production of progeny virus and plaque formation are irreversibly abolished (Fig. 1). This is different from the morphogenesis arrest caused by rifampin, in which reversibility can be obtained even at late times after infection (21, 22). Since the onset of 21- to 23-kDa protein synthesis in cells infected with VVindA17L under permissive conditions occurs at 6 to 8 hpi (Fig. 2A), it seems likely that the reversibility is dependent on the maintenance of 21- to 23-kDa temporal pattern of expression. This finding might suggest that in order to be functional in the morphogenesis process, the 21- to 23-kDa protein should be cotranslationally associated to other viral protein(s) or to nascent viral structures. In this regard, we have previously reported that the 21-kDa product generated by proteolytic processing of the 23-kDa precursor interacts with the 14-kDa envelope protein and that this 14-

FIG. 6. Immunoelectron microscopy localization of the 21- to 23-kDa protein in cells infected with VVindA17L late after induction of the A17L gene with IPTG. Immunolabeling of the 21- to 23-kDa protein was done with the antiserum against the C-terminal peptide (aa 193 to 203), except in panel D, which shows the results with the anti-21- to 23-kDa protein antiserum obtained against a larger C-terminal fragment (aa 136 to 203). (A) After 18 h with IPTG, numerous large viral factories (F) are detected in infected cells. The 21- to 23-kDa protein localizes in the crescent-shaped membranes of the factories (arrowheads). (B) In IVs, the protein is localized in the periphery of the viral particle, where it associates with the membranes. (C) IV-like particles with a less electron-dense periphery are also frequently seen, and in these structures, the protein is located in a more internal position, clearly separated from the surface of the virion. (D) In IMVs, the protein remains associated to the viral membranes. (E and F) Exposure of the 21- to 23-kDa protein on the surface of purified IMVs. The population of virions showed a clear heterogeneity, since a 78% of the virions exhibit a weak or very weak reactivity (arrows in E), while 12% of the virions showed an intense surface signal (F). The same antiserum strongly reacts with IVs on sections of infected cells, but in most of the IMVs (G) or EEVs (H), the signal associated to the 21-kDa protein is lost. mi, mitochondria. Bars, 200 nm.

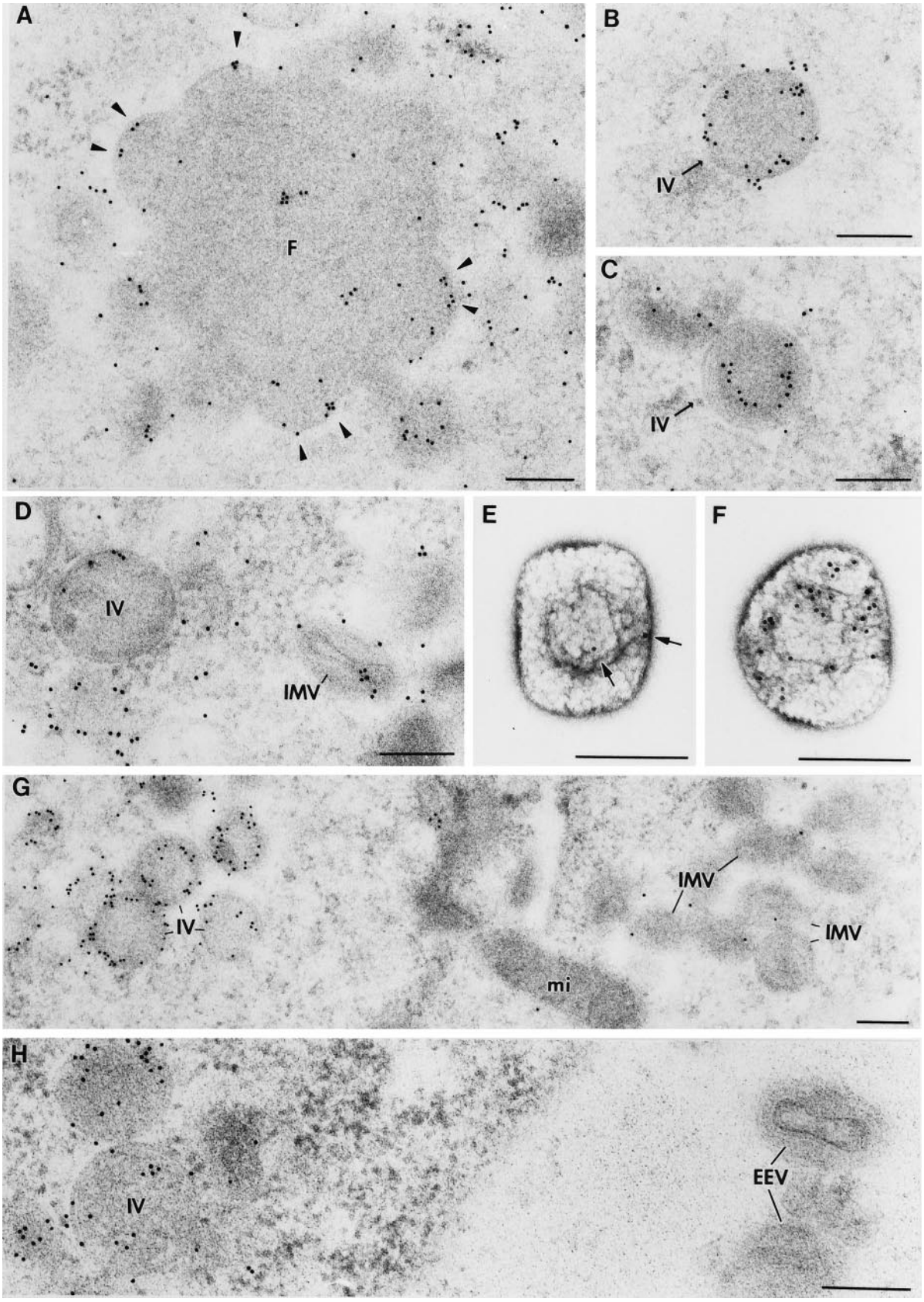
A
F
B
IV
C
IV
D
IV
IMV
E
F
G
IV
IMV
IMV
mi
H
IV
EEV

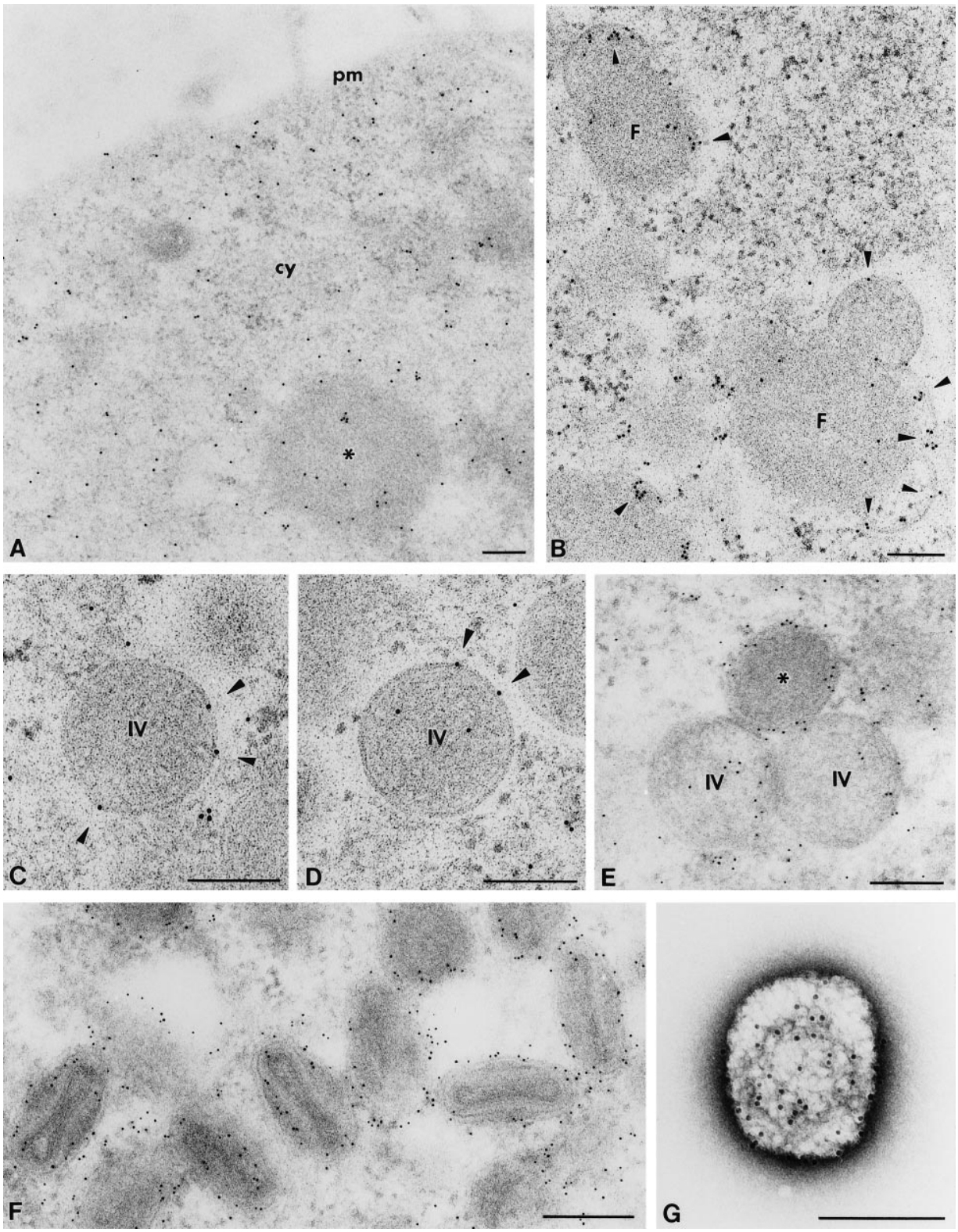

FIG. 7. Immunoelectron microscopy localization of the 14-kDa protein in cells infected with VVindA17L and in purified virions. (A) In infected cells maintained 24 h in the absence of the inducer (IPTG), the 14-kDa protein is dispersed throughout the cytoplasm and in low amounts around or inside the electron-dense dense structures similar to rifampin bodies (asterisk). (B) In infected cells that were treated with the inducer at 6 hpi during a 4-h period, the 14-kDa protein starts to associate (arrowheads) to the crescent-shaped membranes of the viral factories (F). (C and D) IVs also incorporate the 14-kDa protein in low amounts (arrowheads). (E) A more electron-dense form of the IV is sometimes observed, and it presents a stronger signal (asterisk) associated with the 14-kDa protein. (F) The incorporation of the 14-kDa protein significantly increases in the membranes of IMVs. (G) The 14-kDa protein is exposed on the surface of IMVs, as revealed by immunogold labeling of purified virions. Immunolabeling was done with a rabbit anti-14-kDa serum and a 10-nm colloidal gold conjugate (A to D and G) and 5-nm gold conjugate (E and F). cy, cytoplasm; pm, plasma membrane. Bars, 200 nm.

kDa–21-kDa protein interaction is a rapid process that occurs as soon as 30 min after 14-kDa protein synthesis (32). Here we show that in cultures kept under nonpermissive conditions for 6 h, 21- to 23-kDa protein synthesis starts immediately after addition of the inducer (Fig. 2A), and by 4 h postinduction, the amount of protein accumulated is almost comparable to that in cultures infected for 8 h in the presence of IPTG (Fig. 2A; compare lanes 9 and 2). However, there is a significant delay in the establishment of the interaction between the 14-kDa envelope protein and the 21-kDa product compared with cells infected under permissive conditions (Fig. 2B). Since interaction occurs between the 14-kDa protein and the cleaved 21-kDa product, it is possible that a delay in the processing step is responsible for the time lag between synthesis of the protein and interaction with the 14-kDa protein. Regulation of proteolytic processing of VV proteins may be altered under these conditions. In this respect, very little is known about the factors that modulate this maturation process in VVs (43, 44), yet the protease(s) responsible has not been identified. Another possibility is that in cells in which the synthesis of these two proteins has been uncoupled by the late induction of 21- to 23-kDa protein expression and viral morphogenesis has been arrested, there is a differential compartmentalization of 14- and 21-kDa proteins. The delay in establishing 14-kDa–21-kDa protein association after synthesis may simply reflect the time required to join the 14-kDa and 21- to 23-kDa proteins after IPTG addition. This possibility was tested by immunofluorescence. In WR-infected cells or in cells infected with VVindA17L under permissive conditions, the 21- to 23-kDa protein concentrates in the areas corresponding to viral factories, but localization of the protein around the nuclear periphery can also be observed. When morphogenesis is arrested by treatment of WR-infected cells with rifampin, the localization of the 21- to 23-kDa protein does not change substantially, although in this case the protein accumulates in the precursors of viral factories termed rifampin bodies.

In WR-infected cells and in cells infected with VVindA17L in the presence of the inducer, the antibody against the 14-kDa protein strongly labeled distinct punctate structures localized around the periphery and inside the cell. These structures seem to correspond to individual IMVs, as has been previously described (36). Also, in agreement with this notion, when assembly was arrested by rifampin, the punctuate peripheral staining clearly diminished, and strong labeling of rifampin bodies was observed instead. However, when morphogenesis was blocked by inhibition of 21- to 23-kDa protein synthesis, the protein appeared completely dispersed throughout the cytoplasm, showing no association with any particular structure. This striking result, confirmed by immunoelectron microscopy (discussed below), agrees with the idea that in the absence of the 21- to 23-kDa protein, the distribution of 14-kDa protein within the cell is altered, and it suggests that association between the 14- and 21-kDa proteins is an early event in the assembly process that appears to be required to drive the 14-kDa protein into viral structures.

Our previous observations of ultrathin sections from Epon-embedded VVindA17L-infected cells showed that in the absence of the 21- to 23-kDa protein, virion morphogenesis was arrested at a stage prior to formation of the characteristic crescent-shaped membranes. Under these conditions, electron-dense structures resembling the rifampin bodies but lacking distinguishable membranes were observed in the cytoplasm of infected cells (31). These results strongly suggest that the 21- to 23-kDa protein may be involved in the formation of viral membranes. A possibility that arises from the work of Sodeik et al. (37) is that the 21- to 23-kDa protein is targeted to the membranes of cellular IC located between the ER and the Golgi apparatus. We have taken advantage of the reversibility of the A17L gene expression system to investigate the trafficking of the 21- to 23-kDa protein by immunoelectron microscopy. Soon after induction of 21- to 23-kDa protein synthesis, the protein is clearly localized in the membranes of RER and in the nuclear envelope. Also, in some other areas of the cytoplasm, although an underneath structure cannot be distinguished, the organized circular distribution exhibited by the 21- to 23-kDa protein suggests that this protein might be associated to smooth-walled membranes probably related to the membranes of the IC. In this regard, parallel work by Krinjse-Locker et al. showed that the 21- to 23-kDa protein colocalizes with GTPase Rab1, which has been described to localize to the membranes of IC (17a).

The 21- to 23-kDa protein also localizes in the periphery of electron-dense structures which are the precursors of the viral factories and subsequently to the nascent crescent-shaped membranes appearing around these structures. In IVs, two distinct patterns of 21- to 23-kDa protein distribution were observed. Most of IVs present the protein associated to the periphery of the particles; however, other IVs which are distinguishable by having a less electron-dense periphery show the protein arranged in an internal layer. These two forms may represent different transition stages in the maturation process. The second form could correspond to a later stage in which separation and internalization of the inner membrane have occurred. However, although it seems unlikely, we cannot exclude the possibility that the two patterns of labeling reflect different angles of sectioning IVs.

The 21- to 23-kDa protein is also detected in the membranes of IMVs when immunolabeled with an antiserum raised against a 67-aa C-terminal peptide. However, an interesting observation was that an antibody against a 10-aa C-terminal peptide of the protein failed to label the IMVs and EEVs while clearly localizing the protein in other viral forms. It was possible that the protein was cleaved at the C terminus as a maturation step in the transition from IV to IMV. However, by Western blot (immunoblot) analysis of purified IMVs, the 21-kDa protein was similarly recognized by this antibody and the antibody raised against the larger C-terminal fragment of the protein (data not shown). Thus, our electron microscopy data strongly suggest that certain epitopes (between aa 193 and 203) of the 21- to 23-kDa protein are masked and become inaccessible to antibodies as a consequence of the maturation process, during the transition from IV to IMV. Major changes in the conformation of the 21- to 23-kDa protein or the interaction with some other protein(s) can be responsible for this masking effect in the C terminus of the protein.

We previously reported that solubilization of 21- to 23-kDa protein from purified mature virions required treatment with a detergent and a reducing agent, and thus we suggested that the protein localized to the envelope, occupying an internal position (32). To address the question of whether the protein localized to the outer or inner membrane of the viral envelope, purified virions were labeled with the antipeptide antibodies, immunogold labeled, and visualized after negative staining. In support of our interpretation, after extensive examination, most of the virions showed a weak signal or no signal at all, and only 12% exhibited a strong signal. This heterogeneous labeling may reflect different degrees of 21- to 23-kDa protein internalization, with a progressive masking of the peptide represented by the C-terminal 10 aa. However, no IMV subpopulations were detected upon labeling another viral protein such as the 14-kDa protein (100% of the virions exhibited a strong surface signal).

By using this reversible inducible system, we have observed that in the absence of the 21- to 23-kDa protein, the 14-kDa protein appears dispersed throughout the cytoplasm, and only after induction of 21- to 23-kDa protein synthesis did the 14-kDa protein become localized in the periphery of the factories, apparently associated to crescent membranes. Thereafter, the 14-kDa protein appears barely associated to the membranes of spherical IVs but clearly accumulates in the periphery of irregularly shaped particles that have been described as representing a transition stage between IV and IMV (36), as well as on the external surface of IMVs. Our results of the sequential localization of the 14-kDa protein suggest that incorporation of the protein into viral structures is an early event in the morphogenesis, although is in the later stages when the protein accumulates in high amounts. In agreement with the notion of an early incorporation of the 14-kDa protein, in a detailed study of 14-kDa protein localization, Sodeik et al. (36) showed that in rifampin-treated cells, the protein associates to the precursor membranes surrounding the rifampin bodies. Similarly, we have observed that both 14- and 21-kDa proteins are associated to the irregularly shaped membranes formed under these conditions (data not shown).

The weak localization of the 14-kDa protein into the earliest viral structures formed could account for the inability to coprecipitate the 14-kDa–21-kDa protein complex at early times after induction, when most of the protein remains free in the cytoplasm. Coprecipitation can be first observed at 4 h postinduction (data not shown), and this coincides with the appearance of IMVs, as observed by electron microscopy. Also, virus growth analysis shows that virus yields start increasing above background levels about 4 h postinduction (data not shown).

All of these results are consistent with the hypothesis that anchorage of the 14-kDa protein into viral structures is mediated by the 21- to 23-kDa protein. However, since viral membranes do not appear to be formed in the absence of 21- to 23-kDa protein, we cannot exclude the possibility that the lack of incorporation of the 14-kDa protein into viral structures is not directly related to the absence of 21- to 23-kDa protein itself but is an indirect effect due to the inability to form membranes under these conditions. Arguing against this view is the fact that another newly identified VV membrane protein locates in the periphery of the electron-dense structures that are formed in cells infected under nonpermissive conditions, showing a distribution similar to that in viral factories although with a less organized pattern (unpublished data).

In summary, our results are in accordance with a model whereby the 21- to 23-kDa protein is synthesized at the ER, from where the protein would be translocated to the membranes of the IC to generate the precursors of the viral membranes. Other viral protein(s) targeted to the IC remain to be identified. Incorporation of p65 protein into these precursor membranes appears to be required for the acquisition of the characteristic convex appearance, and it has been proposed that p65 acts as an internal scaffold (38). In addition, phosphorylation of an as yet unidentified substrate(s) might be an essential function in the initial steps of the morphogenesis process that could be required for the formation of viral membranes (39, 42). The 14-kDa envelope protein would then become posttranslationally associated to viral membranes through its interaction with the 21-kDa protein. It is possible that C-terminal 10 aa of the 21- to 23-kDa protein are involved in this interaction between the 21- and 14-kDa proteins. This could explain why antibodies to this peptide neither immunoprecipitate the complex and nor label IMVs in sections of infected cells. Competition with the synthetic peptide covering these 10 aa in coprecipitation experiments may help to answer this question.

The reversible virus system characterized in this investigation constitutes a valuable tool with which to synchronize VV morphogenesis at an early stage and provides the basis for studying the trafficking of other viral proteins.

ACKNOWLEDGMENTS

This work was supported by a grant from Comisión Interministerial de Ciencia y Tecnología (CICYT) BIO92-0401 (M. Esteban) and by grant PB91-0109 from the Dirección General de Investigación Científica y Técnica (J. L. Carrascosa). D. Rodríguez was the recipient of a contract from the CSIC-Fundación Ramón Areces. C. Risco and J. R. Rodríguez were recipients of contracts from the MEC of Spain.

We thank J. P. Albar for the production of the 21- to 23-kDa synthetic peptide and I. Poveda and A. Sanz for the photography work. We also thank Victoria Jimenez for her skillful technical assistance.

REFERENCES

1. **Appleyard, G., A. J. Hapel, and E. A. Boulter.** 1971. An antigenic difference between intracellular and extracellular rabbitpox virus. J. Gen. Virol. **13:**9–17.
2. **Blasco, R., and B. Moss.** 1991. Extracellular vaccinia virus formation and cell-to-cell virus transmission are prevented by deletion of the gene encoding the 37,000-dalton outer envelope protein. J. Virol. **65:**5910–5920.
3. **Blasco, R., J. R. Sisler, and B. Moss.** 1993. Dissociation of progeny vaccinia virus from the cell membrane is regulated by a viral envelope glycoprotein: effect of a point mutation in the lectin homology domain of the A34R gene. J. Virol. **67:**3319–3325.
4. **Boulter, E. A., and G. Appleyard.** 1973. Differences between extracellular and intracellular forms of poxviruses and their implications. Prog. Med. Virol. **16:**86–108.
5. **Dales, S., and B. G. T. Pogo.** 1981. Biology of poxviruses. Virol. Monogr. **18:**54–64.
6. **Dales, S., and L. Siminovitch.** 1961. The development of vaccinia virus in Earles L strain cells as examined by electron microscopy. J. Biophys. Biochem. Cytol. **10:**475–503.
7. **Demkowicz, W. E., J.-S. Maa, and M. Esteban.** 1992. Identification and characterization of vaccinia virus genes encoding proteins that are highly antigenic in animals and are immunodominant in vaccinated humans. J. Virol. **66:**386–398.
8. **Duncan, S. A., and G. L. Smith.** 1992. Identification and characterization of an extracellular envelope glycoprotein affecting vaccinia virus egress. J. Virol. **66:**1610–1621.
9. **Engelstad, M., S. T. Howard, and G. L. Smith.** 1992. A constitutively expressed vaccinia gene encodes a 42-kDa glycoprotein related to complement control factors that forms part of the extracellular virus envelope. Virology **188:**801–810.
10. **Engelstad, M., and G. L. Smith.** 1993. The vaccinia virus 42-KDa envelope protein is required for the envelopment and egress of extracellular virus and for virus virulence. Virology **194:**627–637.
11. **Ericsson, M., S. Cudmore, S. Shuman, R. C. Condit, G. Griffiths, J. Krijnse-Locker.** 1995. Characterization of ts16, a temperature-sensitive mutant of vaccinia virus. J. Virol. **69:**7072–7086.
12. **Esteban, M.** 1977. Rifampicin and vaccinia DNA. J. Virol. **21:**796–801.
13. **Grimley, P. M., E. N. Rosemblum, S. J. Mims, and B. Moss.** 1970. Interruption by rifampicin of an early stage in vaccinia virus morphogenesis: accumulation of membranes which are precursors of virus envelopes. J. Virol. **6:**519–533.
14. **Ichihashi, Y., S. Matsumoto, and S. Dales.** 1971. Biogenesis of poxviruses: role of A-type inclusions and host cell membranes in virus dissemination. Virology **46:**507–532.
15. **Isaacs, S. N., E. J. Wolffe, L. G. Payne, and B. Moss.** 1992. Characterization of a vaccinia virus-encoded 42-kilodalton class I membrane glycoprotein component of the extracellular virus envelope. J. Virol. **66:**7217–7224.
16. **Kane, E. M., and S. Shuman.** 1993. Vaccinia virus morphogenesis is blocked by a temperature-sensitive mutation in the I7 gene that encodes a virion component. J. Virol. **67:**2689–2698.
17. **Katz, E., and B. Moss.** 1970. Formation of a vaccinia virus structural polypeptide from a higher molecular weight precursor: inhibition by rifampicin. Proc. Natl. Acad. Sci. USA **66:**677–684.

17a. **Krinjse-Locker, J., S. Schleich, D. Rodriguez, B. Gould, E. J. Snijder, and G. Griffiths.** 1996. The role of a 21-kDa viral membrane protein in the assembly of vaccinia virus from the intermediate compartment. J. Biol. Chem. **271:**14950–14958.

18. **McNulty-Kowalczyk, A., and E. Paoletti.** 1993. Mutations in ORF D13L and other genetic loci alter the rifampicin phenotype of vaccinia virus. Virology **194:**638–646.

19. **Moss, B.** Poxviridae and their replication, p. 2079–2111. *In* B. N. Fields and D. M. Knipe (ed.), Virology, 2nd ed. Raven Press, New York.
20. **Moss, B., and E. N. Rosenblum.** 1973. Protein cleavage and poxvirus morphogenesis: tryptic peptide analysis of core precursors accumulated by blocking assembly with rifampicin. J. Mol. Biol. **81:**267–269.
21. **Moss, B., E. N. Rosenblum, and E. Katz.** 1969. Rifampin: a specific inhibitor of vaccinia virus assembly. Nature (London) **224:**1280–1284.
22. **Nagayama, A., B. G. T. Pogo, and S. Dales.** 1970. Biogenesis of vaccinia: separation of early stages from maturation by means of rifampicin. Virology **4:**1039–1051.
23. **Parkinson, J. E., and G. L. Smith.** 1994. Vaccinia virus gene A36R encodes a Mr 43-50 K protein on the surface of extracellular enveloped virus. Virology **204:**376–390.
24. **Payne, L. G.** 1978. Polypeptide composition of extracellular enveloped vaccinia virus. J. Virol. **27:**28–37.
25. **Payne, L. G.** 1979. Identification of the vaccinia hemagglutinin polypeptide from a cell system yielding large amounts of extracellular enveloped virus. J. Virol. **31:**147–155.
26. **Payne, L. G.** 1980. Significance of extracellular enveloped virus in the in vitro and in vivo dissemination of vaccinia. J. Gen. Virol. **50:**89–100.
27. **Payne, L. G., and K. Kristensson.** 1985. Extracellular release of enveloped vaccinia virus from mouse nasal epithelial cells in vivo. J. Gen. Virol. **66:** 643–646.
28. **Ravanello, M. P., and D. Hruby.** 1994. Conditional lethal expression of the vaccinia virus L1R myristylated protein reveals a role in virion assembly. J. Virol. **68:**6401–6410.
29. **Risco, C., I. M. Antón, C. Suñé, A. M. Pedregosa, J. M. Martín-Alonso, F. Parra, J. L. Carrascosa, and L. Enjuanes.** 1995. Membrane protein molecules of transmissible gastroenteritis coronavirus also expose the carboxy-terminal region on the external surface of the virion. J. Virol. **69:**5269–5277.
30. **Risco, C., L. Menéndez-Arias, T. D. Copeland, P. Pinto da Silva, and S. Oroszlan.** 1995. Intracellular transport of the murine leukemia virus during acute infection of NIH 3T3 cells: nuclear import of nucleocapsid protein and integrase. J. Cell Sci. **108:**3039–3050.
31. **Rodríguez, D., M. Esteban, and J.-R. Rodríguez.** 1995. Vaccinia virus A17L gene product is essential for an early step in virion morphogenesis. J. Virol. **69:**4640–4648.
32. **Rodríguez, D., J.-R. Rodríguez, and M. Esteban.** 1993. The vaccinia virus 14-kilodalton fusion protein forms a stable complex with the processed protein encoded by the vaccinia virus A17L gene. J. Virol. **67:**3435–3440.
33. **Rodríguez, J. F., and G. L. Smith.** 1990. IPTG-dependent vaccinia virus: identification of a virus protein enabling virion envelopment by Golgi membrane and egress. Nucleic Acids Res. **18:**5347–5351.
34. **Schmelz, M., B. Sodeik, M. Ericsson, E. J. Wolffe, H. Shida, G. Hiller, and G. Griffiths.** 1994. Assembly of vaccinia virus: the second wrapping cisterna is derived from the trans Golgi network. J. Virol. **68:**130–147.
35. **Schmutz, C., L. G. Payne, J. Gubser, and R. Wittek.** 1991. A mutation in the gene encoding the vaccinia virus 37,000-M_r protein confers resistance to an inhibitor of virus envelopment and release. J. Virol. **65:**3435–3442.
36. **Sodeik, B., S. Cudmore, M. Ericsson, M. Esteban, E. G. Niles, and G. Griffiths.** 1995. Assembly of vaccinia virus: incorporation of p14 and p32 into the membrane of the intracellular mature virus. J. Virol. **69:**3560–3574.
37. **Sodeik, B., R. W. Doms, M. Ericsson, G. Hiller, C. E. Machamer, W. van't Hof, G. van Meer, B. Moss, and G. Griffiths.** 1993. Assembly of vaccinia virus: role of the intermediate compartment between the endoplasmic reticulum and the Golgi stacks. J. Cell Biol. **121:**521–541.
38. **Sodeik, B., G. Griffiths, M. Ericsson, B. Moss, and R. W. Doms.** 1994. Assembly of vaccinia virus: effects of rifampin on the intracellular distribution of viral protein p65. J. Virol. **68:**1103–1114.
39. **Taktman, P., A. Caligiuri, S. A. Jesty, and U. Sankar.** 1995. Temperature-sensitive mutants with lesions in the vaccinia virus F10 kinase undergo arrest at the earliest stage of virion morphogenesis. J. Virol. **69:**6581–6587.
40. **Tartaglia, J., and E. Paoletti.** 1985. Physical mapping and DNA sequence analysis of the rifampin resistance locus in vaccinia virus. Virology **147:**394–404.
41. **VanSlyke, J. K., P. Lee, E. M. Wilson, and D. E. Hruby.** 1993. Isolation and analysis of vaccinia virus previrions. Virus Genes **7:**311–324.
42. **Wang, S., and S. Shuman.** 1995. Vaccinia virus morphogenesis is blocked by temperature-sensitive mutations in the F10 gene, which encodes protein kinase 2. J. Virol. **69:**6376–6388.
43. **Whitehead, S. S., and D. E. Hruby.** 1994. Differential utilization of a conserved motif for the proteolytic maturation of vaccinia virus proteins. Virology **200:**154–161.
44. **Whitehead, S. S., and D. E. Hruby.** 1994. Transcriptionally controlled *trans*-processing assay: putative identification of a vaccinia virus-encoded proteinase which cleaves precursor protein p25. J. Virol. **68:**7603–7608.
45. **Wilcock, D., and G. L. Smith.** 1994. Vaccinia virus core protein VP8 is required for virus infectivity, but not for core protein processing or for INV and EEV formation. Virology **202:**294–304.
46. **Wolffe, E. J., S. N. Isaacs, and B. Moss.** 1993. Deletion of the vaccinia virus B5R gene encoding a 42-kilodalton membrane glycoprotein inhibits extracellular virus envelope formation and dissemination. J. Virol. **67:**4732–4741.
47. **Wolffe, E. J., D. M. Moore, P. J. Peters, and B. Moss.** 1996. Vaccinia virus A17L open reading frame encodes an essential component of nascent viral membranes that is required to initiate morphogenesis. J. Virol. **70:**2797–2808.
48. **Zhang, Y., and B. Moss.** 1991. Vaccinia virus morphogenesis is interrupted when expression of the gene encoding an 11-kilodalton phosphorylated protein is prevented by the *Escherichia coli lac* repressor. J. Virol. **65:**6101–6110.
49. **Zhang, Y., and B. Moss.** 1992. Immature viral envelope formation is interrupted at the same stage by lac operator-mediated repression of the vaccinia virus D13L gene and by the drug rifampicin. Virology **187:**643–653.